References

[1] Kojima M, Hosoda H, Date Y, Nakazato M, Matsuo H, Kangawa K. Ghrelin is a growth hormone-releasing acylated peptide from stomach. Nature 1999;402: 656–60.

[2] Date Y, Kojima M, Hosoda H, Sawaguchi A, Mondal MS, Suganuma T, et al. Ghrelin, a novel growth hormone-releasing acylated peptide, is synthesized in a distinct endocrine cell type in the gastrointestinal tracts of rats and humans. Endocrinology 2000;141:4255–61.

[3] Wren AM, Small CJ, Ward HL, Murphy KG, Dakin CL, Taheri S, et al. The novel hypothalamic peptide ghrelin stimulates food intake and growth hormone secretion. Endocrinology 2000;141:4325–8.

[4] Wren AM, Small CJ, Fribbens CV, Neary NM, Ward HL, Seal LJ, et al. The hypothalamic mechanisms of the hypophysiotropic action of ghrelin. Neuroendocrinology 2002;76:316–24.

[5] Nagaya N, Moriya J, Yasumura Y, Uematsu M, Ono F, Shimizu W, et al. Effects of ghrelin administration on left ventricular function, exercise capacity, and muscle wasting in patients with chronic heart failure. Circulation 2004;110:3674–9.

[6] Nagaya N, Itoh T, Murakami S, Oya H, Uematsu M, Miyatake K, et al. Treatment of cachexia with ghrelin in patients with COPD. Chest 2005;128:1187–93.

[7] Miljic D, Pekic S, Djurovic M, Doknic M, Milic N, Casanueva FF, et al. Ghrelin has partial or no effect on appetite, growth hormone, prolactin, and cortisol release in patients with anorexia nervosa. J Clin Endocrinol Metab 2006;91:1491–5.

[8] Strasser F, Lutz TA, Maeder MT, Thuerlimann B, Bueche D, Tschöp M, et al. Safety, tolerability and pharmacokinetics of intravenous ghrelin for cancer-related anorexia/cachexia: a randomized, placebo-controlled, double-blind, double-crossover study. Br J Cancer 2008;98:300–8.

[9] DeBoer MD. Emergence of ghrelin as a treatment for cachexia syndromes. Nutrition 2008;24:806–14.

[10] Deboer MD, Zhu X, Levasseur PR, Inui A, Hu Z, Han G, et al. Ghrelin treatment of chronic kidney disease: improvements in lean body mass and cytokine profile. Endocrinology 2008;149:827–35.

[11] Howard AD, Feighner SD, Cully DF, Arena JP, Liberator PA, Rosenblum CI, et al. A receptor in pituitary and hypothalamus that functions in growth hormone release. Science 1996;273:974–7.

[12] Wang HJ, Geller F, Dempfle A, Schäuble N, Friedel S, Lichtner P, et al. Ghrelin receptor gene: identification of several sequence variants in extremely obese children and adolescents, healthy normal-weight and underweight students, and children with short normal stature. J Clin Endocrinol Metab 2004;89:157–62.

[13] Pantel J, Legendre M, Cabrol S, Hilal L, Hajaji Y, Morisset S, et al. Loss of constitutive activity of the growth hormone secretagogue receptor in familial short stature. J Clin Invest 2006;116:760–8.

[14] Pantel J, Legendre M, Nivot S, Morisset S, Vie-Luton MP, le Bouc Y, et al. Recessive isolated growth hormone deficiency and mutations in the ghrelin receptor. J Clin Endocrinol Metab 2009;94:4334–41.

[15] Holst B, Frimurer TM, Mokrosinski J, Halkjaer T, Cullberg KB, Underwood CR, et al. Overlapping binding site for the endogenous agonist, small-molecule agonists, and ago-allosteric modulators on the ghrelin receptor. Mol Pharmacol 2009;75: 44–59.

[16] Floquet N, M'Kadmi C, Perahia D, Gagne D, Berge G, Marie J, et al. Activation of the ghrelin receptor is described by a privileged collective motion: a model for constitutive and agonist-induced activation of a sub-class A G protein-coupled receptor (GPCR). J Mol Biol 2010;395:769–84.

[17] Coulie B, Matsuura B, Dong M, Hadac EM, Pinon DI, Feighner SD, et al. Identification of peptide ligand-binding domains within the human motilin receptor using photoaffinity labeling. J Biol Chem 2001;276:35518–22.

[18] Matsuura B, Dong M, Coulie B, Pinon DI, Miller LJ. Demonstration of a specific site of covalent labeling of the human motilin receptor using a biologically active photolabile motilin analog. J Pharmacol Exp Ther 2005;313:1101–8.

[19] Matsuura B, Dong M, Miller LJ. Differential determinants for peptide and non-peptidyl ligand binding to the motilin receptor. J Biol Chem 2002;277:9834–9.

[20] Matsuura B, Dong M, Naik S, Miller LJ, Onji M. Differential contributions of motilin receptor extracellular domains for peptide and non-peptidyl agonist binding and activity. J Biol Chem 2006;281:12390–6.

[21] Tokunaga H, Matsuura B, Dong M, Miller LJ, Ueda T, Furukawa S, et al. Mutational analysis of predicted intracellular loop domains of human motilin receptor. Am J Physiol Gastrointest Liver Physiol 2008;294:G460–6.

[22] Feighner SD, Tan CP, McKee KK, Palyha OC, Hreniuk DL, Pong SS, et al. Receptor for motilin identified in the human gastrointestinal system. Science 1999;284:2184–8.

[23] Holst B, Cygankiewicz A, Jensen TH, Ankersen M, Schwartz TW. High constitutive signaling of the ghrelin receptor – identification of a potent inverse agonist. Mol Endocrinol 2003;17:2201–10.

[24] Feighner SD, Howard AD, Prendergast K, Palyha OC, Hreniuk DL, Nargund R, et al. Structural requirements for the activation of the human growth hormone secretagogue receptor by peptide and nonpeptide secretagogues. Mol Endocrinol 1998;12:137–45.

[25] Grynkiewicz G, Poenie M, Tsien RY. A new generation of calcium indicators with greatly improved fluorescence properties. J Biol Chem 1985;260:3440–50.

[26] Munson PJ, Rodbard D. LIGAND: a versatile computerized approach for characterization of ligand-binding systems. Anal Biochem 1980;107:220–39.

[27] Kolakowski LF. GCRDb: a G protein-coupled receptor database. Recept Channels 1994;2:1–7.

[28] Holliday ND, Holst B, Rodionova EA, Schwartz TW, Cox HM. Importance of constitutive activity and arrestin-independent mechanisms for intracellular trafficking of the ghrelin receptor. Mol Endocrinol 2007;21:3100–12.

[29] Guan XM, Yu H, Palyha OC, McKee KK, Feighner SD, Sirinathsinghji DJ, et al. Distribution of mRNA encoding the growth hormone secretagogue receptor in brain and peripheral tissues. Brain Res Mol Brain Res 1997;48:23–9.

[30] Gnanapavan S, Kola B, Bustin SA, Morris DG, McGee P, Fairclough P, et al. The tissue distribution of the mRNA of ghrelin and subtypes of its receptor, GHS-R, in humans. J Clin Endocrinol Metab 2002;87:2988.

[31] Takeshita E, Matsuura B, Dong M, Miller LJ, Matsui H, Onji M. Molecular characterization and distribution of motilin family receptors in the human gastrointestinal tract. J Gastroenterol 2006;41:223–30.

JOURNAL OF VIRAL HEPATITIS

Journal of Viral Hepatitis, 2011, 18, 200–205 doi:10.1111/j.1365-2893.2010.01300.x

Mechanism of restoration of immune responses of patients with chronic hepatitis B during lamivudine therapy: increased antigen processing and presentation by dendritic cells

S. M. F. Akbar,[1,2] N. Horiike,[2] S. Chen,[2] K. Michitaka,[2] M. Abe,[2] Y. Hiasa,[2] B. Matsuura[2] and M. Onji[2] [1]*Department of Medical Sciences, Toshiba General Hospital, Tokyo;* [2]*Department of Gastroenterology and Metabology, Ehime University Graduate School of Medicine, Ehime, Japan*

Received September 2009; accepted for publication January 2010

SUMMARY. Restoration of host immunity has been reported in patients with chronic hepatitis B (CHB) after treatment with lamivudine; however, the underlying mechanisms of this treatment have not been determined. This study examined the role of antigen-presenting dendritic cells (DC) in restoration of host immunity. Circulating DC were isolated from peripheral blood of 23 patients with CHB before and 1, 3, and 12 months after starting lamivudine therapy. The non-antigen-specific proliferation of DC was assessed in allogenic mixed leucocyte reaction. Dendritic cells were cultured with hepatitis B surface antigen (HBsAg) to prepare HBsAg-pulsed DC. Proliferative capacity and production of interleukin (IL)-12 and interferon (IFN)-γ of HBsAg-pulsed DC were evaluated. Circulating unpulsed DC and HBsAg-pulsed DC showed significantly higher levels of T-cell proliferation capacities 1 month after lamivudine therapy compared to proliferation levels before therapy ($P < 0.05$). HBsAg-pulsed DC also produced significantly higher levels of IL-12 and IFN-γ with lamivudine therapy compared to levels before therapy ($P < 0.05$). HBsAg-pulsed DC from lamivudine-treated patients induced proliferation of T cells of patients with CHB in an antigen-specific manner ($P < 0.05$). However, T-cell stimulatory capacity of DC did not increase significantly 3 and 12 months after lamivudine therapy compared to 1 month after lamivudine therapy. Immune restoration as a result of lamivudine therapy is regulated at least in part by activation of DC. However, progressive activation of DC was not seen as treatment duration progressed, indicating the limitations of this mechanism of viral clearance.

Keywords: chronic hepatitis B, dendritic cells, immune restoration, lamivudine.

INTRODUCTION

Chronic hepatitis B virus (HBV) infection is a major cause of morbidity and mortality worldwide. Of 350 million people chronically infected with HBV globally, considerable numbers develop chronic hepatitis B (CHB) and its complications, such as liver cirrhosis, liver failure, and hepatocellular carcinoma. Approximately, 0.5–1.2 million people die annually because of HBV-related diseases [1]. A study by Perz *et al.* has shown that chronic HBV infection likely accounts for the majority of both cirrhosis and hepatocellular carcinoma globally and in all regions of the world [2]. Treatment is recommended for patients with CHB so that complications can be minimized or delayed. The main goal of antiviral therapy is to suppress HBV replication and induce remission of liver disease. The ultimate goal of therapy is to prevent cirrhosis, hepatic failure, and hepatocellular carcinoma [3].

The number of medications that can treat CHB is increasing. Based on their mechanism of action, two types of antiviral agents have been approved or are in clinical development: (i) immune modulators (interferon alpha-2b, pegylated interferon-2a and interferon alpha-2a) and (ii) viral polymerase inhibitors that belong to the nucleoside and nucleotide analogue family.

Nucleoside analogues are well tolerated, less expensive than interferon, and can be administered orally. Accordingly, nucleoside analogues are now used widely around the world, especially in developing countries, where more than 90% of patients infected with chronic HBV reside. Nucleoside

Abbreviations: CHB, chronic hepatitis B; CPM, counts per minute; DC, dendritic cells; HBsAg, hepatitis B surface antigen; HBV, hepatitis B virus; MLR, mixed leucocyte reaction; PBMC, Peripheral blood mononuclear cells.

Correspondence: S. M. F. Akbar, MD, PhD, Principal Investigator, Department of Medical Sciences, Toshiba General Hospital, 6-3-22 Higashi Oi, Shinagawa, Tokyo 140-8522, Japan. E-mail: sheikh.akbar@po.toshiba.co.jp

analogues are potent inhibitors of HBV replication in CHB. However, several studies have shown that these agents have immune modulator capacities in patients with CHB. Boni *et al.* showed that lamivudine treatment restores T-cell responsiveness [4]. Lamivudine has also been reported to overcome cytotoxic T-cell hyporesponsiveness in CHB [5]. Recently, Cooksley *et al.* showed that adefovir dipivoxil treatment caused increased $CD4^+$ -cells responses in patients with CHB compared to placebo [6]. Restoration of T lymphocyte subpopulation has been detected in patients with CHB treated with entecavir [7]. A study by Evans *et al.* has shown immune modulator capacities of telbivudine in patients with CHB [8].

These findings support the idea that in addition to having potent antiviral capacity, nucleoside analogues can also modulate host immunity in patients with CHB. However, almost nothing is known about the mechanism of immune restoration or immune induction capacities of nucleoside analogues. Proper insights about different cellular and molecular events regarding immune modulator capacities of nucleoside analogues may contribute to development of more potent therapeutic regimens for CHB.

The primary aim of this study was to dissect the mechanisms underlying the immune modulator capacities of lamivudine, the most commonly used nucleoside analogue. We focused on the functions of antigen-presenting dendritic cells (DC), initiators, and regulators of immune responses [9–12]. This was carried out for two principal reasons. First, DC regulate both innate and antigen-specific immunity in situ. DC infiltrate to the site of viral localization, produce critical mediators of innate immunity, and ultimately recognize, process, and present viral antigens for induction of antigenic-specific immunity [9–12]. Second, DC function has been reported to be decreased and impaired in patients with CHB mainly because of increased HBV load, high levels of HBV-related antigens, and localization of HBV DNA in DC [13–15]. Thus, it is possible that immune restoration of patients with CHB during lamivudine therapy may be mediated through DC. Accordingly, we examined DC function in patients with CHB before and after lamivudine therapy.

MATERIALS AND METHODS

Twenty-three patients with lamivudine-naïve CHB were enrolled in this study. Clinical profiles of the patients are shown in Table 1. All patients had chronic liver disease and attended our university hospital for periodic monitoring and therapy. The diagnosis of CHB was made based on clinical symptoms and liver function tests. In 20 patients, the final diagnosis of CHB was confirmed by histologic evaluation of the liver biopsy specimen. All patients were positive for HBsAg and HBV DNA in the sera. They also exhibited exacerbation and remission of liver disease during the last 6 months. Concomitant infection and super-infection with hepatitis A virus, hepatitis C virus, cytomegalovirus,

Table 1 Clinical profiles of patients

Parameters	
Number of patients	23
Age (mean and range)	42 ± 12.2 (range: 23–70 years)
Sex (Male : Female)	16:7
Alanine aminotransferase (U/L)	157 ± 52
HBV DNA (log genomic equivalent)	6.8 ± 1.3
HBeAg + patients	13
Anti-HBe + patient	10
Liver histology	
Hepatitis	
Mild	6
Moderate	10
Severe	4
Level of fibrosis	
F1	6
F2	2
F3	7
F4	5

Data are mean and standard deviation. Liver biopsy specimens were available in 20 patients with chronic hepatitis B.

Epstein–Barr virus, or herpes simplex virus were ruled out serologically or molecularly. All patients with CHB were provided with oral lamivudine at a dose of 100 mg once daily. The nature and possible consequences of this study were explained to all patients, and all of them gave written informed consent to receive lamivudine therapy. The studies have been performed according to the World Medical Association Declaration of Helsinki, and the procedures have been approved by the local Ethics Committee of Ehime University, Japan.

Study design

Whole blood was collected from patients with CHB just before the start of lamivudine therapy. In addition, whole blood was collected 1, 3, and 12 months after therapy began. The functions of T lymphocytes, monocyte-derived DC, and circulating DC were assessed. In some patients, immunocyte function was evaluated serially.

Estimation of HBV markers

The presence of HBsAg and antibody to HBsAg (anti-HBs) in the sera was determined using chemiluminescent immunoassay kits (Architect™ HBsAg and Architect™ anti-HBs, Dainabot, Tokyo, Japan). Levels of HBeAg and anti-HBe were determined using enzyme immunoassay kits (AxSYM™ HBeAg Assay and AxSYM™ HBeAg Assay, Dainabot). HBV DNA in sera was assayed with a commercial kit (DNA probe

'Chugai-HBV', Chugai Diagnostic Science Co., Ltd., Tokyo, Japan), and levels were expressed as log genomic equivalent (LGE/mL) (limit of HBV DNA detection >3.7 LGE/mL).

Isolation of T lymphocytes and DC from peripheral blood

Peripheral blood mononuclear cells (PBMC) from patients with CHB were isolated by density gradient separation using Ficoll-Conray (Pharmacia, San Jose, CA, USA) and were resuspended in RPMI 1640 (Iwaki, Chiba, Japan) plus 10% heat-inactivated foetal calf serum (Filtron Pty., Ltd., Brooklyn, Australia) containing L-glutamine and gentamycin. Cell viability was checked by the trypan blue exclusion (0.1% trypan blue) test.

Circulating DC were isolated from PBMC by two-step immunomagnetic cell sorting using a commercial kit (DC Isolation Kit, Miltenyi Biotech GmbH, Bergisch Gladbach, Germany), according to the manufacturer's instructions and as described previously [16,17]. Briefly, T cells, monocytes, and natural killer cells were depleted from PBMC using magnetic beads coated with monoclonal antibodies against CD3 (clone BW264/56), CD11b (clone M1/70.15.11.5), and CD16 (clone VEP-13) by Auto MACS (Miltenyi Biotech Gmbh). Purified populations of circulating DC were isolated from the depleted cell fractions by a positive selection step using a monoclonal antibody against CD4 (clone M-T321, Miltenyi Biotech Gmbh). Flow cytometric analysis revealed <1.0% contaminating T lymphocytes, B lymphocytes, and natural killer cells in circulating DC.

In some experiments, monocyte-derived DC were prepared by culturing PBMC with granulocyte-macrophages stimulating factor (800 U/mL) and interleukin (IL)-4 (400 U/mL) (Pepro Tech EC Ltd., London, UK) for 7 days. DC were retrieved from the culture and washed for three times with phosphate-buffered saline (PBS) as described elsewhere [18].

T lymphocytes were isolated from PBMC of one normal volunteer or patient with CHB using an affinity column (Collect™, Biotex Laboratories INC, Edmonton, Canada) in which B cells were depleted from PBMC during their passage through the affinity column containing polyclonal goat anti-human IgG (H + L) [16]. Flow cytometric analysis revealed that the purity of T-cell populations was >95%.

Expression of MHC/HLA antigen and costimulatory antigens on circulating DC

The expressions of MHC class II (HLA DR), MHC class I (HLA A, B, C), CD86, and CD40 on circulating DC were assessed by direct flow cytometry using fluorescein isothiocyanate-conjugated monoclonal antibody to human HLA DR (MHC class II, Clone L243), HLA A, B, C (MHC class I), and phycoerythrin-conjugated monoclonal antibody to human CD86 (clone 2331 [FUN-1]) and CD40 (all from BD Pharmingen, San Jose, CA, USA). Data acquisition and analysis were performed on a fluorescein-activated cell sorter (Becton Dickinson Biosciences, San Jose, CA, USA).

Production of HBsAg-pulsed DC

To produce HBsAg-pulsed DC, blood DC were cultured with a recombinant HBsAg (Tokyo Institute of Immunology, Tokyo, Japan) for 48 h. After the end of culture, DC were pelleted and washed five times in PBS. After the last wash, the final wash solutions were collected and preserved at −20 °C to assess whether there was any free HBsAg in HBsAg-pulsed DC [18].

Lymphoproliferative assays

We optimized the culture condition of allogenic mixed leucocyte reaction (MLR) and antigen-specific lymphoproliferation by conducting a series of preliminary experiments as described in previous studies [17]. T cells (2×10^5) from allogenic normal controls or patients with CHB were cultured with γ-irradiated (40 Gy, HILTEX Co., Ltd., HW-150, Osaka, Japan) DC or HBsAg-pulsed DC (1×10^4) for 5 days at 37 °C in a humidified incubator containing 5% CO_2 in air. The levels of incorporation of [^{3}H]-thymidine during the last 12 h of the 5-day culture were determined in a liquid scintillation counter (Beckman LS 6500; Beckman Instruments, Inc., Fullerton, CA, USA) as counts per minute (CPM). All assays were performed in 96-well plates and the mean CPM of at least 12 wells calculated. Stimulation index was measured by dividing the levels of CPM in culture containing stimulants with the levels of CPM in control cultures.

Cytokine production assays

The allogenic MLR was performed for 5 days without adding [^{3}H]-thymidine to the cultures. HBsAg-pulsed DC were cultured for 2 days. The supernatants were collected and centrifuged. Levels of IL-12 and IFN-γ in the supernatants were measured by an enzyme-linked immunosorbent assay using a commercial kit (BD Pharmingen) [17].

Statistical analysis

Values are as mean ± standard deviation (SD). Data were analysed by unpaired t tests if data were normally distributed and by Mann–Whitney rank-sum test if they were skewed. Differences were considered significant if $P < 0.05$.

RESULTS

Circulating DC expressed DC-related markers such as HLA A, B, C, HLA DR, and CD86. The proportion of contaminating lymphocytes, natural killer cells, and monocytes were <5% in circulating DC. The functionality of DC was assessed in

allogenic MLR. DC induced proliferation of allogenic T cells in a dose-dependent manner (data not shown).

Increased proliferation of T lymphocytes from patients with CHB because of lamivudine therapy

Mean levels of Con A-induced T-cell proliferation were significantly higher in samples collected 1 month after lamivudine therapy (stimulation index: 147.8 ± 22.1) compared to before treatment (stimulation index: 51.2 ± 11.5) ($P < 0.05$). However, the proliferative capacity of T lymphocytes did not show any further increases at 3 months after therapy started (stimulation index: 130.9 ± 25.6) ($P > 0.05$). We also checked Con A-induced T-cell proliferation 12 months after the start of lamivudine therapy. Levels of proliferation of T cells (stimulation index: 127.3 ± 37.3) did not show any significant changes compared to levels after 1 month of lamivudine therapy (stimulation index: 147.8 ± 22.1) ($P > 0.05$).

Increased T-cell proliferation capacities of circulating DC from patients with CHB during lamivudine therapy

The proliferative capacities of DC were increased in patients with CHB because of lamivudine therapy. T-cell stimulatory capacities of circulating DC of all patients with CHB were estimated 1 and 3 months after therapy started. Levels of blastogenesis (assessed from stimulation index values) were significantly higher ($P < 0.05$) in cultures containing DC from patients with CHB 1 month after therapy (stimulation index: 90.3 ± 15.6) started compared to before treatment (stimulation index: 45.3 ± 10.0). Similarly, circulating DC from patients with CHB 3 months after therapy started showed significantly higher levels of T-cell proliferation compared to DC before therapy (stimulation index: 90.4 ± 14.3) (Fig. 1). However, the proliferative capacity of DC did not show any significant difference between samples at 1 and 3 months after therapy started (Fig. 1).

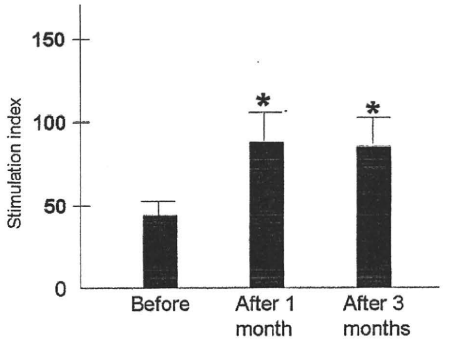

Fig. 1 Increased proliferation of allogenic T cells by DC from lamivudine-treated patients with CHB. Data are mean and standard deviation. $P < 0.05$ compared to before therapy.

Kinetics of proliferation capacities of DC because of lamivudine therapy

We checked the proliferation capacities of DC serially before, and 1, 3, and 12 months after therapy started in six patients. The proliferative capacity of DC increased significantly (before therapy versus 1 month after therapy; stimulation index 44.2 ± 123 versus stimulation index, 105.2 ± 18.2) ($P < 0.05$) 1 month after lamivudine therapy started, but did not show any significant increase during the next 11 months, although patients were receiving lamivudine on a daily basis (Fig. 2).

Increased production of IL-12 and IFN-γ in allogenic MLR culture containing DC from patients with CHB 1 month after therapy started

Levels of IL-12 and IFN-γ were significantly higher in allogenic MLR culture supernatants containing DC from lamivudine-treated CHB 1 month after start of therapy compared to cultures containing DC from pretreated patients ($P < 0.05$) (Table 2).

Increased cytokine production and antigen processing and presentation capacity of DC because of lamivudine therapy

DC from patients with CHB were pulsed with HBsAg before and 1 and 3 months after lamivudine therapy. These DC were cultured for 48 h to assess their production of two critical cytokines required for immune responses: IL-12 and IFN-γ. As shown in Fig. 3, levels of IFN-γ were significantly increased in culture containing HBsAg-pulsed DC from patients with CHB 1 month (76.4 ± 8.3 pg/mL) and 3 months after lamivudine therapy (73.9 ± 8.8 pg/mL) compared to HBsAg-pulsed DC before therapy (36.5 ± 13.7 pg/mL) ($P < 0.05$). Similarly, levels of IL-12 were significantly increased in culture containing HBsAg-pulsed DC from patients with CHB 1 month (181.8 ± 32.7 pg/mL) and 3 months after lamivudine therapy (187.7 ± 33.1 pg/mL) compared to HBsAg-pulsed DC before therapy (111.4 ± 25.4 pg/mL) ($P < 0.05$). The levels of these cytokines were

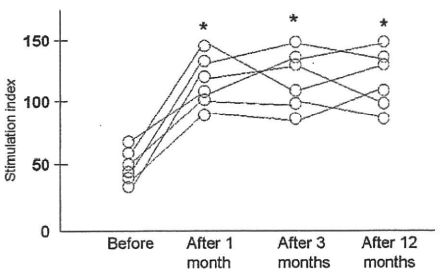

Fig. 2 Kinetics of DC function before and after lamivudine therapy. Data are shown as stimulation index of six individual cases. $P < 0.05$ compared to before therapy.

Table 2 Increased cytokine production by DC in patients with chronic hepatitis B before and after treatment with lamivudine

	Interleukin-12 (pg/mL)	Interferon-γ (pg/mL)
Before lamivudine therapy	45 ± 6	32 ± 5
1 month after lamivudine therapy	354 ± 45*	167 ± 29*

Data are mean and standard deviation.
*$P < 0.05$, compared to culture containing DC before therapy.

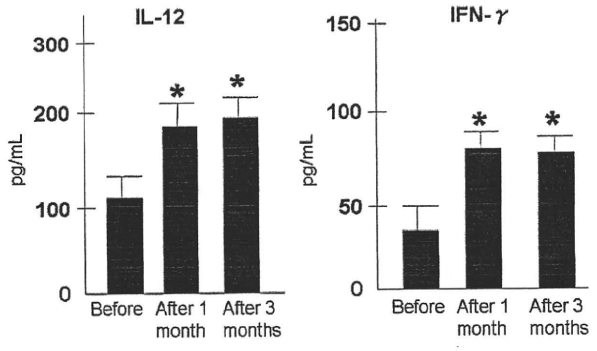

Fig. 3 Increased IL-12 and INF-γ production by HBsAg-pulsed DC from patients with CHB after lamivudine therapy. Data are mean and standard deviation. $P < 0.05$ compared to before therapy.

almost comparable in culture containing HBsAg-pulsed DC from patients with CHB 1 and 3 months after lamivudine therapy (Fig. 3).

Increased T-cell activation capacity of HBsAg-pulsed DC from lamivudine-treated patients with CHB

DC were isolated before and 1 month after the start of lamivudine therapy. These DC were cultured with HBsAg to produce HBsAg-pulsed DC. As shown in Fig. 4, HBsAg-pulsed DC from patients with CHB before lamivudine therapy could not induce proliferation of autologous T cells *in vitro*. However, HBsAg-pulsed DC from lamivudine-treated patients with CHB induced proliferation of T cells from patients with CHB (Fig. 4).

DISCUSSION

Restoring T-cell responsiveness and overcoming cytotoxic T-cell (CTL) hyporesponsiveness have been reported in patients with CHB treated with lamivudine therapy [4,5]. In addition, restoration of immune responses by adefovir, entecavir, and telbivudine has also been reported [6–8]. However, the

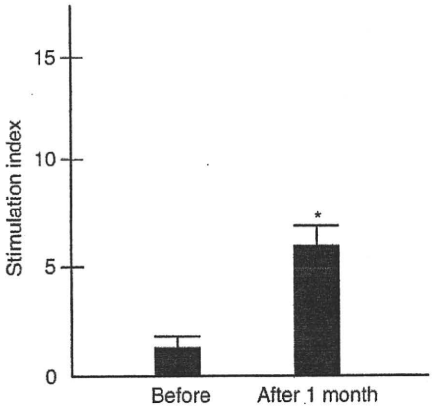

Fig. 4 Increased T-cell proliferation capacity of HBsAg-pulsed DC before and 1 month after start of lamivudine therapy. $P < 0.05$ compared to before therapy.

mechanism underlying this immune restoration by nucleoside analogues in patients with CHB is not understood, although these drugs mainly block or reduce replication of the HBV. Reduction of HBV DNA and downregulation of HBV-related proteins with lamivudine treatment may be one of the factors that lead to restoration of immune responses in patients with CHB. HBV DNA and HBV-related antigens may have a dominant role in impaired HBV-specific immunity in patients with CHB. However, other factors may be related to immune restoration because of nucleoside treatment, and further characterization of these events is essential.

In this study, we showed increased proliferative capacities of DC in a non-antigen-specific (allogenic MLR stimulation) manner as well as in an antigen-specific manner (HBsAg-pulsed DC activation). In addition, lamivudine treatment induced increased cytokine production from DC. However, the functional capacity of DC was not increased with time because DC from lamivudine-treated patients 3 or 12 months after lamivudine intake did not show increased activity compared to 1 month after treatment.

These findings may have important clinical implications. Boni *et al.* found transient restoration of immune responses with lamivudine [4,5]. Their study showed a transient increase in HBV-specific CD4 and CD8 responses, but these effects were not sustained over time. We found similar results regarding DC activation. It is probable that further activation of DC may be required to attain sustained antiviral activity with lamivudine. Also, DC function should be monitored in HBsAg-positive, HBV DNA-negative, and treatment-naïve patients in future to develop insights about role of HBV replication on DC function.

Understanding the biochemical and molecular targets of lamivudine and other nucleoside analogues may lead to new therapeutic strategies against chronic HBV infection. Lamivudine treatment caused transient increases in DC function, but not progressive activation of DC. This effect can be

achieved by adding an immune modulator. The combination of lamivudine with an immune modulator has shown efficient antiviral potential, but, their role in modulation of ultimate clinical outcome is not so promising [19–22]. In large randomized phase III studies comparing lamivudine and peginterferon monotherapy and the combination of peginterferon and lamivudine in HBeAg-positive and HBeAg-negative patients, combination therapy was associated with a more profound decrease in viral load, compared with either monotherapy. However, no significant difference was observed in treatment end points such as viral suppression, HBeAg seroconversion, and HBsAg clearance between peginterferon monotherapy and combination therapy.

In addition to interferon, lamivudine has been used with HBsAg-based prophylactic vaccine or IL-12 to improve the clinical outcome in patients with CHB. However, the capacities of these drugs to restore immune responses, especially HBV-specific immune responses, have not been properly elucidated. Although we found that lamivudine caused transient increased HBsAg-specific immunity in patients with CHB, the persistence of this effect needs to be examined in future studies. Addition of appropriate immune modulators with lamivudine may induce progressive stimulation of DC and potent restoration of antigen-specific immunity in patients with CHB. Also, the function of capacity of DC should be assessed when these patients switch to another antiviral in future.

REFERENCES

1 Ganem D, Prince AM. Hepatitis B virus infection-natural history and clinical consequences. *N Engl J Med* 2004; 350: 1118–1129.

2 Perz JF, Armstrong GL, Farrington LA, Huttin YJF, Bell BP. The contributions of hepatitis B virus and hepatitis C virus infections to cirrhosis and primary liver cancer worldwide. *J Hepatol* 2006; 45: 529–538.

3 Lok AS, McMohan BJ. Chronic hepatitis B. *Hepatology* 2007; 45: 507–539.

4 Boni C, Bertoletti A, Penna A *et al.* Lamivudine treatment can restore T cell responsiveness in chronic hepatitis B. *J Clin Invest* 1998; 102: 968–975.

5 Boni C, Penna A, Ogg GS *et al.* Lamivudine treatment can overcome cytotoxic T-cell hyporesponsiveness in chronic hepatitis B: new perspectives for immune therapy. *Hepatology* 2001; 33: 963–971.

6 Cooksley H, Chokshi S, Maayan Y *et al.* Hepatitis B virus e antigen loss during adefovir dipivoxil therapy is associated with enhanced virus-specific CD4+ T-cell reactivity. *Antimicrob Agents Chemother* 2008; 52: 312–320.

7 You J, Sriplung H, Geater A *et al.* Impact of viral replication inhibition by entecavir on peripheral T lymphocyte subpopulations in chronic hepatitis B patients. *BMC Infect Dis* 2008; 8: 123. (http://www.biomedcentral.com/1471-2334/8/123).

8 Evans A, Riva A, Cooksley H *et al.* Programmed death 1 expression during antiviral treatment of chronic hepatitis B: impact of hepatitis B e-antigen seroconversion. *Hepatology* 2008; 48: 759–769.

9 Steinman RM. Dendritic cells: understanding immunogenicity. *Eur J Immunol* 2007; 37(Suppl 1): S53–S60.

10 Onji M, Akbar SM. Dendritic Cells in Clinics. Tokyo: Springer, 2008.

11 Banchereau J, Paluka K. Dendritic cells as therapeutic vaccines against cancer. *Nat Rev Immunol* 2005; 3: 296–306.

12 Mellman I, Steinman RM. Dendritic cells: specialized and regulated antigen processing machines. *Cell* 2001; 106: 255–258.

13 Op den Brouw ML, Binda RS, van Roosmalen MH *et al.* Hepatitis B virus surface antigen impairs myeloid dendritic cell function: a possible immune escape mechanism of hepatitis B virus. *Immunology* 2009; 126: 280–289.

14 Hasebe A, Akbar SM, Furukawa S, Horiike N, Onji M. Impaired functional capacities of liver dendritic cells from murine hepatitis B virus (HBV) carriers: relevance to low HBV-specific immune responses. *Clin Exp Immunol* 2005; 139: 35–42.

15 Duan XZ, Wang M, Li HW, Zhuang H, Xu D, Wang FS. Decreased frequency and function of circulating plasmocytoid dendritic cells (pDC) in hepatitis B virus infected humans. *J Clin Immunol* 2004; 24: 637–646.

16 Wertheimer AM, Bakke A, Rosen HR. Direct enumeration and functional assessment of circulating dendritic cells in patients with liver disease. *Hepatology* 2004; 40: 335–345.

17 Tsubouchi E, Akbar SM, Murakami H, Horiike N, Onji M. Isolation and functional analysis of circulating dendritic cells from hepatitis C virus (HCV) RNA-positive and HCV RNA-negative patients with chronic hepatitis C: role of antiviral therapy. *Clin Exp Immunol* 2004; 137: 417–423.

18 Akbar SM, Furukawa S, Yoshida O, Hiasa Y, Horiike N, Onji M. Induction of anti-HBs in HB vaccine nonresponders *in vivo* by hepatitis B surface antigen-pulsed blood dendritic cells. *J Hepatol* 2007; 47: 60–66.

19 Janssen HL, van Zonneveld M, Senturk H *et al.* Pegylated interferon alfa-2b alone or in combination with lamivudine for HBeAg-positive chronic hepatitis B: a randomised trial. *Lancet* 2005; 365: 123–129.

20 Lau GK, Piratvisuth T, Luo KX *et al.* Peginterferon alfa-2a, lamivudine, and the combination for HBeAg-positive chronic hepatitis B. *N Engl J Med* 2005; 352: 2682–2695.

21 Marcellin P, Lau GK, Bonino F *et al.* Peginterferon alfa-2a alone, lamivudine alone, and the two in combination in patients with HBeAg-negative chronic hepatitis B. *N Engl J Med* 2004; 351: 1206–1217.

22 Vandepapelière P, Lau GK, Leroux-Roels G *et al.* Therapeutic vaccination of chronic hepatitis B patients with virus suppression by antiviral therapy: a randomized, controlled study of co-administration of HBsAg/AS02 candidate vaccine and lamivudine. *Vaccine* 2007; 25: 8585–8597.

J Gastroenterol (2010) 45:859–867
DOI 10.1007/s00535-010-0218-4

ORIGINAL ARTICLE—LIVER, PANCREAS, AND BILIARY TRACT

Impaired dendritic cell functions disrupt antigen-specific adaptive immune responses in mice with nonalcoholic fatty liver disease

Teruki Miyake · Sheikh Mohammad Fazle Akbar · Osamu Yoshida · Shiyi Chen · Yoichi Hiasa · Bunzo Matsuura · Masanori Abe · Morikazu Onji

Received: 17 September 2009 / Accepted: 29 January 2010 / Published online: 2 March 2010

Abstract
Background/aims The magnitude of antigen-specific immunity was assessed in a murine model of nonalcoholic fatty liver diseases (NAFLD). Because antigen-specific immunity was diminished in NAFLD mice, the underlying mechanisms were evaluated through analysis of the functions of antigen-presenting dendritic cells (DC) and other immunocytes.
Methods For 12 weeks, NAFLD mice received a high-fat (60%) and high-calorie (520 kcal/100 g) diet. C57BL/6 mice (controls) received a standard diet. NAFLD mice and control mice were immunized with hepatitis B vaccine containing hepatitis B surface antigen (HBsAg) and hepatitis B core antigen (HBcAg). Antibody to HBsAg (anti-HBs), HBsAg and HBcAg-specific cellular immune response and functions of whole spleen cells, T lymphocytes, B lymphocytes and spleen DCs of NAFLD and control mice were assessed in vitro.
Results Levels of anti-HBs and the magnitude of proliferation of HBsAg and HBcAg-specific lymphocytes were significantly lower in NAFLD mice than control mice ($P < 0.05$). The spleen cells of NAFLD mice produced significantly higher levels of inflammatory cytokines ($P < 0.05$) and exhibited significantly increased T cell proliferation compared with control mice ($P < 0.05$). However, the antigen processing and presenting capacities of spleen DCs were significantly decreased in NAFLD mice compared with control mice ($P < 0.05$). Palmitic acid, a saturated fatty acid, caused diminished antigen processing and presenting capacity of both murine and human DCs.
Conclusions Nonalcoholic fatty liver disease mice exhibit decreased magnitudes of antigen-specific humoral and cellular immune responses. This effect is mainly, if not solely, due to impaired antigen processing and presentation capacities of DC.

Keywords NAFLD · Adaptive immunity · Dendritic cell · HB vaccine

T. Miyake · S. M. F. Akbar · O. Yoshida · S. Chen · Y. Hiasa · B. Matsuura · M. Abe · M. Onji (✉)
Department of Gastroenterology and Metabology, Ehime University Graduate School of Medicine, Toon, Ehime 791-0295, Japan
e-mail: onjimori@m.ehime-u.ac.jp

S. M. F. Akbar
Department of Medical Sciences, Toshiba General Hospital, Tokyo, Japan

Introduction

Obesity and its associated conditions, including nonalcoholic fatty liver disease (NAFLD), have reached worldwide epidemic proportions. The pathological spectrum of NAFLD extends from simple hepatic steatosis to nonalcoholic steatohepatitis to liver cirrhosis. In addition to liver-related complications, patients with NAFLD are more prone to develop insulin resistance, type 2 diabetes mellitus and coronary heart disease [1, 2].

Different metabolic factors, such as over-nutrition, oxidative stress, mitochondrial injury and fatty acid lipotoxicity, are related to the pathogenesis of NAFLD [3]. Recent studies have shown the role of the immune system in NAFLD because some comorbidities associated with NAFLD, such as insulin resistance and type 2 diabetes mellitus, may be triggered by increased activation of the

cells of the immune system [4, 5]. Excessive production of tumor necrosis factor alpha (TNF-α) and interferon-gamma (IFN-γ), and activation of cells of innate immune responses have been reported in NAFLD [4–11].

However, little has been published about antigen-specific adaptive immunity in NAFLD, although epidemiologic data indicate that adaptive immunity may be compromised in these subjects. NAFLD patients are susceptible to infection and exhibit reduced responses to vaccinations [12, 13]. In addition, many NAFLD patients are also chronically infected with hepatitis B virus and hepatitis C virus [14, 15]. Because impaired virus-specific adaptive immunity is responsible for chronic infection with these viruses [16], NAFLD may also be characterized by distorted antigen-specific adaptive immunity.

Exacerbated innate immunity and possible impaired adaptive immunity in NAFLD led us to assess antigen-specific immune responses in a murine model of NAFLD. Our study showed that in comparison to control mice, antigen-specific humoral and cellular immune responses were significantly reduced in NAFLD mice. Interestingly, impaired antigen-specific immune responses in NAFLD mice were detected in the presence of increased inflammatory cytokines and exacerbated T and B lymphocyte function. Because antigen-presenting dendritic cells (DC) are initiators and regulators of the antigen-specific immune responses [17–19], we examined the functional capacities of DCs in NAFLD mice. Finally, we also checked the impacts of fatty acids on the functional capacities of human peripheral blood mononuclear cells (PBMCs) and DCs to evaluate clinical implications of our study in NAFLD mice.

Materials and methods

Mice

Seven-week-old male C57BL/6J mice were purchased from Nihon Clea (Tokyo, Japan). Mice were housed individually in polycarbonate cages in our laboratory facilities and maintained in a temperature- and humidity-controlled room (23 ± 1°C) with a 12-h light/dark cycle. After 1 week, one group of mice was given a high-fat diet (HFD) that consisted of 20% protein, 20% carbohydrate and 60% fat with an energy density of 520 kcal/100 g (D12492, RESEARCH DIETS, Inc., New Brunswick, NJ). Control mice were fed a standard laboratory chow that contained 26% protein, 60% carbohydrate and 13% fat with an energy density of 360 kcal/100 g. All mice received humane care, and the study protocol was approved by the Ethical Committee of the Graduate School of Medicine, Ehime University, Japan.

Human volunteers

Ten normal human volunteers (age range, 26–55 years) were enrolled in this study. They were healthy and free from any evidence of liver disease, autoimmune disease and infectious disease. Informed consent was obtained from each volunteer included in the study, and the study protocol conforms to the ethical guidelines of the 1975 Declaration of Helsinki as reflected in a prior approval by the institution's human research committee (no. 16-1, dated 2004-02-26).

Assessment of biochemical and histological parameters

Blood glucose levels (Glucose PILOT; Aventir Biotech, LLC, Carlsbad, CA), serum insulin concentrations (Insulin kit, Morinaga, Yokohama, Japan), and serum triglyceride and cholesterol levels (Wako Pure Chemical Industries, Ltd., Osaka, Japan) were measured by commercially available kits. We measured fatty acid concentrations in mice sera by liquid chromatography (Shikoku Chuken, Matsuyama, Japan).

Mice were anesthetized with diethyl ether and killed by cervical dislocation. The weight of the liver, spleen and fatty tissue were measured. Histological assessment of fatty liver was done by histochemistry.

Based on body weight, extent of fatty liver, levels of blood glucose, serum cholesterol and insulin levels, a mice model of NAFLD occurred 12 weeks after study start.

Immunization schedule

Nonalcoholic fatty liver disease mice and control mice were immunized once with intraperitoneal hepatitis B (HB) vaccine containing hepatitis B surface antigen (HBsAg, 1, 2 and 4 μg) (Heptavax-II, subtype adw, Banyu Pharmaceutical). Mice were also injected with hepatitis B core antigen (HBcAg; 1, 2 and 4 μg) (Tokyo Institute of Immunology, Tokyo, Japan).

Assessment of humoral immune response to HBsAg

The levels of antibodies to HBsAg (anti-HBs) in sera were measured 4 weeks after immunization by chemiluminescence enzyme immunoassay method (Shikoku Chuken, Matsuyama, Japan) as described previously [20]. Values were expressed as mIU/ml.

Isolation of T lymphocytes, B lymphocytes and DC

Different immunocytes from mice spleen were isolated as described previously [21–23]. In short, single cell suspensions of spleen were prepared and suspended in RPMI 1640

(Iwaki, Osaka, Japan) containing 10% fetal calf serum (Filtron PTY LTD, Brooklyn, Australia). T lymphocytes and B lymphocytes were purified from single cell suspensions of spleen using T lymphocyte and B lymphocyte isolation kits (Miltenyi Biotec, GmbH, Bergisch Gladbach, Germany) as described previously [20]. DCs were isolated from single cell suspensions of spleen by density column (specific gravity 1.082), plastic adherence, re-culture on plastic surface, and depletion of macrophages and lymphocytes [21].

Peripheral blood mononuclear cells were isolated from human blood by density centrifugation on Ficoll-hypaque (specific gravity 1.077). DCs were also isolated from PBMC by plastic adherence and culturing with granulocyte-macrophages colony-stimulating factor and interleukin (IL)-4, as described in our previous report [24].

Cytokine production by different immunocytes

Immunocytes from mice were cultured with concanavalin A (Con A, Sigma Chemical, St. Louis, MO), lipopolysaccharides (LPS, Sigma Chemical), cytosine-phosphate-guanosine oligodeoxynucleotide (CPG-ODN) (InvivoGen, San Diego, CA) and polyinosinic polycytidylic acid (poly I:C) (Sigma Chemical) for 48 h to assess production of cytokines.

Measurements of palmitic acid and oleic acid for culture experiments

In some experiments, palmitic acid and oleic acid were added to cultures to assess their impact on cytokine production from human PBMC and also to assess if these fatty acids have any role on antigen processing and presentation capacities of DC. In short, fatty acids were solubilized in ethanol with albumin as stock solution of 20 mM and stored at −20°C, as described previously [25, 26]. Fatty acid-albumin complex solutions were freshly prepared before each experiment. The pH was adjusted to 7.4. Subsequently, we performed preliminary experiments using 10–1000 μM of fatty acids to assess the concentrations of fatty acids that would not compromise cell viability. As cell viability was not compromised when 50–100 μM of fatty acid was used in any of the 10 preliminary experiments, we used 50 μM of fatty acid for assessing the effect of palmitic acid and oleic acid for co-culture experiments.

Preparation of HBsAg-specific and HBcAg-specific memory lymphocytes

Eight-week-old male C57BL/6 mice were immunized twice with HB vaccine containing 10 μg of HBsAg at an interval of 4 weeks or 10 μg of HBcAg. Serial evaluation revealed that at 7–8 months after immunization, antigen-specific lymphocytes in these mice were in a memory state, because these lymphocytes proliferated after stimulation with DCs and antigen, but not with antigen alone [27].

Preparation of HBsAg-pulsed DC

Spleen DCs or human blood DCs (1–2 million) suspended in 1.0 ml of RPMI 1640 plus 10% fetal calf serum were cultured with 50 μg of HBsAg or 50 μg of HBcAg (Institute of Immunology) for 48 h [24, 27]. DCs were recovered from the cultures and washed five times with phosphate-buffered saline. In some studies, palmitic acid and oleic acid (suspended in albumin) were added to cultures during preparation of antigen-pulsed murine spleen DCs and human blood DCs.

Lymphoproliferative assays

We conducted a series of experiments to optimize the protocols for the lymphocyte proliferation assays as described previously [20–24, 27]. T lymphocytes and B lymphocytes were cultured with or without polyclonal activators for 72 h to assess the proliferative capacities of these immunocytes.

Dendritic cells from NAFLD mice and control mice were cultured with T cells from these mice to assess the proliferative capacities of autologous and syngenic lymphocytes in vitro.

Lymphocytes from HBsAg-based vaccine-injected mice and HBcAg-immunized mice were cultured in the presence or absence of recombinant HBsAg or HBcAg for 120 h to evaluate antigen-specific cellular immune responses. Unpulsed DCs or antigen-pulsed DCs were cultured with antigen-specific memory lymphocytes for 120 h to assess the functional capacity of DC.

All cultures were performed in 96-well U-bottom plates (Corning, Tokyo, Japan). [^{3}H]-Thymidine (1.0 mCi/L, Amersham Biosciences UK LTD, Buckinghamshire, UK) was diluted in sterile phosphate-buffered saline and added to the cultures. Cells were harvested automatically by a multiple cell harvester (LABO MASH, Futaba Medical, Tokyo, Japan) after 16 h onto a filter paper (LM 101–10, Futaba Medical). The level of incorporation of ^{3}[H]-thymidine was determined in a liquid scintillation counter (Beckman-LS 5000, Beckman Instruments INC, Fullerton, CA). Data were expressed as count per minute (CPM) or stimulation index. Stimulation index was counted by dividing the levels of CPM in culture containing antigen with the levels of CPM in control cultures.

Estimation of cytokines

Levels of different cytokines in culture supernatants were estimated using a commercial kit for the cytometric bead array method as described previously [20, 27]. Levels of cytokines in culture supernatants were calibrated from the mean fluorescence intensities of the standard negative control, standard positive control and samples by Cytometric Bead Array software (BD Biosciences Pharmingen, San Jose, CA) using a Macintosh computer (SAS Institute, Cary, NC).

Statistical analysis

Values are presented as mean ± standard error of mean (SEM). Data were analyzed by unpaired t tests if data were normally distributed and by Mann-Whitney rank-sum test if they were skewed. Differences were considered significant at $P < 0.05$.

Results

Characteristics of NAFLD mice

On the basis of data from preliminary experiments, we assessed different parameters of HFD-consuming mice and control mice 12 weeks after study commencement. As shown in Fig. 1a, the body weight of both groups of mice was similar at the start of experiments. However, 12 weeks after study commencement, the body weight of HFD mice was significantly higher than that of control mice ($P < 0.05$). Concentrations of fasting blood sugar, blood insulin and serum cholesterol levels, as well as the weights of total fatty tissues, were also significantly ($P < 0.05$) increased in HFD mice compared with control mice (Fig. 1b–e). In addition, the weights of the liver, spleen, and subcutaneous and visceral fat were significantly increased in HFD mice compared with control mice ($P < 0.05$) (data not shown). Levels of different fatty acids were significantly ($P < 0.05$) increased in the sera of HFD-consuming mice 12 weeks after study commencement. Levels of palmitic acid and oleic acid are shown in Fig. 2a. Histological assessment revealed severe fatty liver at 12 weeks after study commencement in HFD mice (Fig. 2b).

Decreased antigen-specific humoral immune responses to HBsAg in NAFLD mice

Levels of anti-HBs in the sera were significantly lower in NAFLD mice compared with control mice due to immunization with 1 μg (levels of anti-HBs in the sera, NAFLD mice versus control mice; 14 ± 6 mIU/ml versus 205 ± 66 mIU/ml, $n = 10$, $p < 0.05$), 2 μg (levels of anti-HBs in the sera, NAFLD mice versus control mice; 17 ± 8 mIU/ml versus 440 ± 72 mIU/ml, $n = 10$, $P < 0.05$) and 4 μg (levels of anti-HBs in the sera, NAFLD mice versus control mice; 107 ± 21 mIU/ml versus 524 ± 99 mIU/ml, $n = 10$, $P < 0.05$).

Decreased antigen-specific cellular immune responses to HBsAg and HBcAg in NAFLD mice

Lymphocytes from all HBsAg and HBcAg-immunized control mice showed significant proliferation when cultured

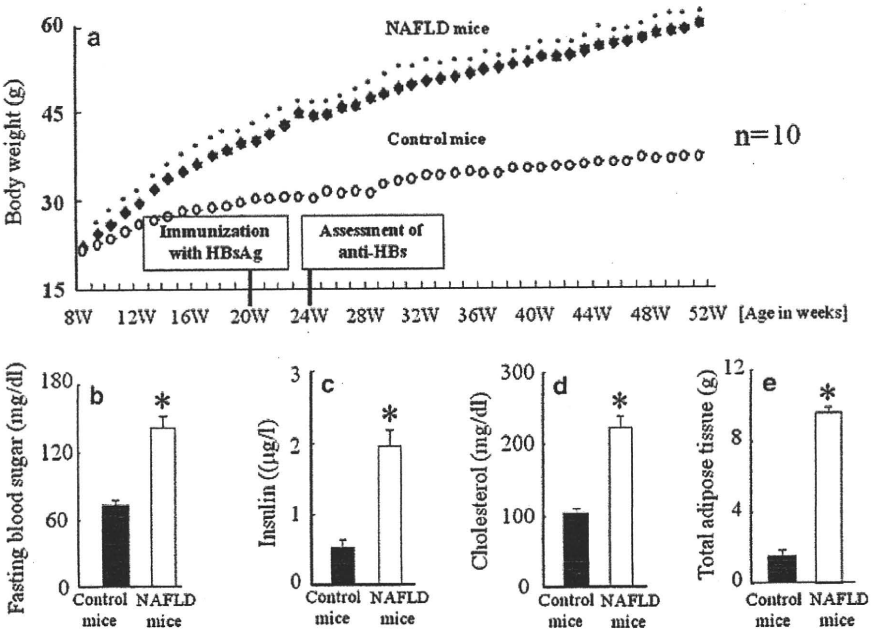

Fig. 1 Characterization of mice with nonalcoholic fatty liver disease (NAFLD). Eight-week-old male C57BL/6 (control) mice were given either a high-fat diet containing 60% fat and 520 kcal/100 g or a standard laboratory chow. The kinetics of weight gain of NAFLD mice and control mice are shown in **a**. Levels of blood sugar, serum insulin and cholesterol, and amounts of total adipose tissues were significantly higher in NAFLD mice compared with control mice ($P < 0.05$) (**b–e**). Data are mean and SEM of body weight of 10 mice in each group. *$P < 0.05$ compared with control mice of same duration

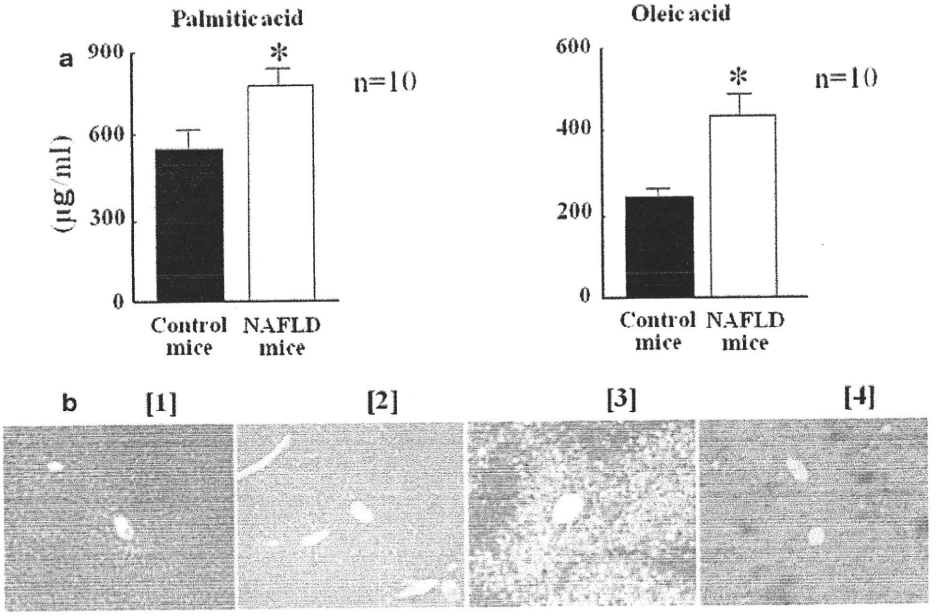

Fig. 2 **a** Increased levels of palmitic acid and oleic acid in the sera of nonalcoholic fatty liver disease (NAFLD) mice. Data are mean and SEM of different parameters of 10 mice in each group. $*P < 0.05$ compared with control mice of same duration. **b** Severe fatty liver of NAFLD mice. Figures in [1] and [2] represent liver specimens from control mice by hematoxylin eosin stain and Sudan III stain, respectively. Figures in [3] and [4] represent hematoxylin eosin stain and Sudan III stain of NAFLD mice, respectively

with different doses of HBsAg (1, 10, and 100 μg/ml) (Fig. 3a) and HBcAg (1, 10, and 100 μg/ml) (Fig. 3b). In contrast, lymphocytes from HBsAg and HBcAg-immunized NAFLD mice exhibited significantly ($P < 0.05$) lower levels of proliferation in cultures stimulated with 1, 10 and 100 μg/ml of HBsAg or 1, 10 and 100 μg/ml of HBcAg compared with control mice (Fig. 3a, b). In fact, lymphocytes from some HBsAg-immunized and HBcAg-immunized lymphocytes did not show significant proliferation due to stimulation by HBsAg or HBcAg.

Increased proliferative capacities of lymphocytes from NAFLD mice

Initially, we assumed that the impaired antigen-specific humoral and cellular immune responses of NAFLD mice might be responsible for the decreased proliferative capacity or cytokine production of lymphocytes of these mice. However, levels of proliferation of T lymphocytes to Con A (Fig. 4a) and B lymphocytes to LPS (Fig. 4b) from NAFLD mice were significantly higher than those from control mice ($P < 0.05$).

In addition, spleen T and B cells from NAFLD mice produced significantly higher levels of inflammatory cytokines (IL-6, TNF-α and IFN-γ) due to stimulation with different polyclonal immune stimulators (Con A, LPS, CPG -ODN and poly I:C) (Fig. 5) compared with those from control mice ($P < 0.05$).

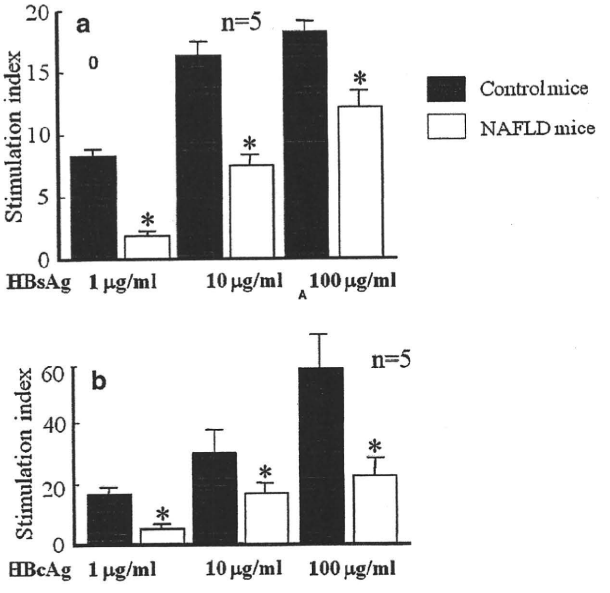

Fig. 3 Decreased antigen-specific immune responses in mice with nonalcoholic fatty liver disease (NAFLD). NAFLD mice ($n = 5$) and control mice ($n = 5$) were immunized with a hepatitis vaccine containing 4 μg of hepatitis B surface antigen (HBsAg) and 4 μg of hepatitis B core antigen (HBcAg). Four weeks after immunization, spleen lymphocytes (2×10^5) were cultured with different recombinant HBsAg and HBcAg for 5 days. Levels of blastogenesis were assessed from incorporation of ^{3}H-thymidine as count per minute (CPM). Data are presented as stimulation index, which was calculated by dividing the levels of CPM in cultures containing HBsAg (**a**) and HBcAg (**b**) with cultures containing no HBsAg or HBcAg. Mean ± SEM of five separate experiments are shown. $*P < 0.05$ compared with control mice

Impaired functional capacities of spleen DCs from NAFLD mice

As the functional capacities of lymphocytes were mostly higher in NAFLD mice, we evaluated the antigen processing and presentation capacities of DCs because they regulate both the induction and effecter phases of antigen-specific immune responses. Spleen DCs from NAFLD mice had significantly reduced capacities to stimulate HBsAg-specific memory lymphocytes (levels of blastogenesis; 3480 ± 67 CPM) compared with DCs from control mice (15823 ± 134 CPM, $n = 5$) ($P < 0.05$). This indicated that DCs of NAFLD mice were less able to process and present HBsAg in culture.

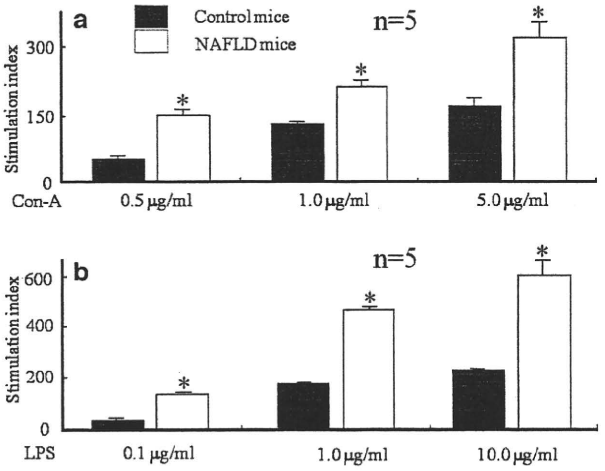

Fig. 4 Increased non-antigen-specific proliferation of T and B lymphocytes from nonalcoholic fatty liver disease (NAFLD) mice to polyclonal antigens. T and B lymphocytes from NAFLD mice and control mice were stimulated with concanavalin A (Con A) (**a**) and lipopolysaccharides (LPS) (**b**), respectively. Levels of proliferation of lymphocytes were assessed from the levels of count per minute in cultures and expressed as the stimulation index, as described in the legend of Fig. 3. Mean and SEM of five separate experiments are shown. *$P < 0.05$ compared with control mice

Defective loading of DCs from NAFLD mice with soluble antigen

To further assess the function of DCs, we produced HBsAg-pulsed DCs and HBcAg-pulsed DCs. These DCs are supposed to activate antigen-specific immunocytes directly. In our study, HBsAg-pulsed DCs and HBcAg-pulsed DCs from NAFLD mice had a significantly lower capacity to stimulate HBsAg-specific (Fig. 6a) and HBcAg-specific lymphocytes (Fig. 6b) compared with those from control mice ($P < 0.05$).

Assessment of impaired DC function of NAFLD mice

The impaired DC function of NAFLD mice could have resulted from negative feedback of increased lymphocyte activity. In order to assess this phenomenon, we cultured DCs from NAFLD mice and control mice with T cells from these mice. The levels of blastogenesis of cultures containing DCs from NAFLD mice with T cells from NAFLD mice and control mice were 35.5 ± 3.2 and 37.4 ± 4.3, respectively

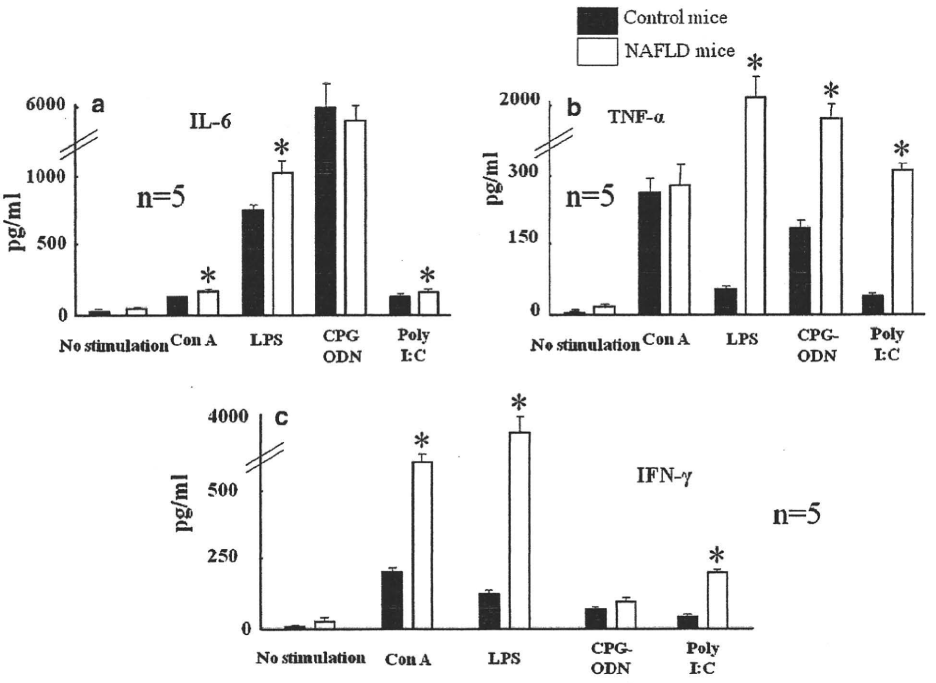

Fig. 5 Increased production of inflammatory cytokines from spleen cells of nonalcoholic fatty liver disease (NAFLD) mice due to stimulation with polyclonal mitogens. Spleen cells from NAFLD mice and control mice were stimulated with concanavalin A (Con A), lipopolysaccharides (LPS), cytosine-phosphate-guanosine oligodeoxynucleotide (CPG-ODN) and polyinosinic polycytidylic acid (poly I:C). Levels of IL-6 (**a**), TNF-α (**b**) and IFN-γ (**c**) were measured in the culture supernatants by the cytometric bead array method. Mean and SEM of five separate experiments are shown. *$P < 0.05$ compared with control mice

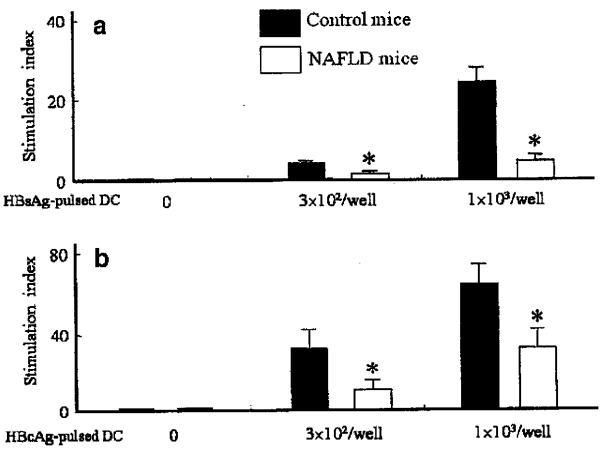

Fig. 6 Decreased capacity of hepatitis B surface antigen (HBsAg)-pulsed (**a**) and HBcAg-pulsed dendritic cells (DCs) (**b**) from nonalcoholic fatty liver disease (NAFLD) mice to activate HBsAg and HBcAg-specific memory lymphocytes in vitro. HBsAg-pulsed DCs and HBcAg-pulsed DCs were challenged to induce proliferation of antigen-specific lymphocytes in vitro. Levels of proliferation of HBsAg-specific and HBcAg-specific lymphocytes without DCs were regarded as a stimulation index of 1.0. Mean and SEM of five separate experiments are shown. $*P < 0.05$ compared with HBsAg-pulsed DC from control mice

(stimulation index of mean and SEM of 5 separate experiments) ($p > 0.05$). On the other hand, the levels of blastogenesis of cultures containing DCs from control mice with T cells from NAFLD mice and control mice were 41.4 ± 2.9 and 46.2 ± 2.2, respectively (stimulation index of mean and SEM of 5 separate experiments) ($p > 0.05$).

Effect of fatty acid on antigen-specific immunity

In spite of an inflammatory microenvironment, DCs from NAFLD mice could not induce proliferation of antigen-specific T cells in vitro. We assumed that some fatty acid may be related to impaired DC function. Levels of different fatty acids in the sera were significantly increased in the sera of NAFLD mice ($P < 0.05$). We decided to assess the effects of palmitic acid and oleic acid on DC function because studies have documented diverse effects of these fatty acids on immune responses [28]. HBsAg-pulsed DCs prepared in the presence of palmitic acid showed significantly lower levels (stimulation index; 1.4 ± 0.3, $n = 3$) of stimulatory capacity compared to HBsAg-pulsed DCs prepared in the presence of oleic acid (stimulation index; 15.8 ± 2.2, $n = 3$) ($p < 0.05$).

Increased cytokine production by human PBMC in presence of palmitic acid

Human PBMCs were cultured with palmitic acid and oleic acid, and levels of cytokines were assessed. Palmitic acid, but not oleic acid, induced significantly higher levels of IL-1β (palmitic acid vs. oleic acid, 1615 ± 300 pg/ml vs. 365 ± 141 pg/ml, $n = 5$) and TNF-α (palmitic acid vs. oleic acid, 828 ± 253 pg/ml vs. 260 ± 97 pg/ml, $n = 5$) from human PBMCs in vitro ($P < 0.05$).

Disruption of antigen processing and presenting capacities of human HBsAg-pulsed DCs cultured in presence of palmitic acid

Human HBsAg-pulsed DCs prepared in the presence of palmitic acid induced significantly lower levels of antigen-specific T cell proliferation in vitro compared with those prepared in the presence of oleic acid (stimulation index, 12.3 ± 1.2 vs. 1.9 ± 0.4, DCs cultured in presence of oleic acid vs. DCs cultured with palmitic acid, $P < 0.05$, $n = 5$).

Restoration of antigen-specific immunity of NAFLD mice after consuming control diet for 8 weeks

To assess if it was possible to reverse the impaired antigen-specific immunity of NAFLD mice by providing them with a control diet, we fed the control diet to NAFLD mice for 8 weeks and immunized them with HBsAg to assess antigen-specific immunity. Providing a normal diet for 8 weeks caused decreased body weight and normalization of different biochemical parameters of NAFLD mice. Interestingly, these mice also produced similar levels of anti-HBs compared with age- and sex-matched control mice (406 ± 93.4 mIU/ml vs. 441 ± 109 mIU/ml, $n = 5$, $P > 0.05$) due to immunization with a HB vaccine containing 2 μg of HBsAg.

Discussion

To develop insights about the nature and magnitudes of adaptive immune responses in NAFLD, we prepared a murine model of NAFLD because many immune-related cellular and molecular events cannot be properly examined in humans due to ethical and technical concerns. Providing a HFD that contained high levels of fat (60%) and a high calorie density (520 kcal/100 g), we realized a murine model of NAFLD after 12 weeks. Spleen cells of NAFLD mice in this study also produced significantly higher levels of proinflammatory cytokines (IL-6, IFN-γ, and TNF-α) compared with control mice that consumed normal laboratory chow. In addition, T and B lymphocytes from NAFLD mice exhibited increased proliferative capacities in response to polyclonal immune modulators compared with control mice.

In spite of an increased activated state of cells with innate immunity, NAFLD mice were almost incapable of

responding to the antigenic challenge for induction of antigen-specific humoral and cellular immune responses. In this study, we used HBsAg and HBcAg for induction of adaptive immunity. Subjects with NAFLD may also induce impaired levels of adaptive immunity in response to challenge with microbes and cancer cells. Presumptive data supporting this have been cited in the literature [29, 30].

In spite of harboring an activated population of lymphocytes and an inflammatory mucosal milieu, impaired antigen processing and presentation of DCs in NAFLD subjects hindered their antigen-specific immunity. This condition is comparable to chronic infections and cancers in which impaired functions of DCs compromise an effective antigen-specific immunity. The functional anomaly of DCs in NAFLD may be induced by various factors. One is related to diet. Palmitic acid, but not oleic acid, caused down-regulation of HBsAg processing and presentation of DCs. Some other fatty acids, especially a saturated fatty acid, may be responsible for impaired DC function in NAFLD. A second possibility of impaired DC function in NAFLD mice may be due to the non-antigen-specific maturation of DCs in these mice. In order to process and present antigen to T cells, DCs need to recognize, internalize, process and present antigens to clonally selected immunocytes. In an inflammatory microenvironment, DCs may undergo activation and maturation prior to recognition, internalization and processing of antigens. Although these DCs produce abundant amounts of cytokines, they are unable to induce activation of antigen-specific immunocytes because of their nature of maturation in a non-antigen-specific manner [17–19]. In fact, diminished antigen-specific immunity due to non-antigen-specific maturation of DCs has been reported by us in a model of Con-A-induced hepatitis [31]. Although we have shown that the saturated fatty acid, palmitic acid, can induce impaired function of DCs, NAFLD mice also had impaired glucose tolerance. This may also contribute to impaired immune responses [32]. In fact, the role of impaired glucose intolerance on adaptive immunity or on the functional capacity of DCs should be well addressed in the future.

Similar results to those in this study in NAFLD mice were also found in humans, as palmitic acid caused increased inflammatory cytokine production and impaired DC function in human DCs in this study. However, further study is needed to confirm these findings in patients with NAFLD.

Interestingly, the immune anomaly of the NAFLD condition was reversed in our model by providing a control diet for 8 weeks. This emphasizes the importance of diet therapy in NAFLD.

In this study, we used two well-characterized antigens of hepatitis B virus (HBV) to induce adaptive immunity in NAFLD mice. Obesity and NAFLD have reached worldwide epidemic proportions. In addition, HBV infection represents a major global public health problem, with 2 billion HBV infections and 350 million chronic HBV carriers. A protective vaccine against the HBV is now available and used extensively around the world. However, little has been explored about the protective capacity of this vaccine in subjects with obesity and NAFLD. Our study indicates the need to re-visit the ongoing protocol of a prophylactic vaccine against HBV. In addition, NAFLD mice also exhibited impaired DC function and adaptive immunity to HBcAg. Taken together, it appears that NAFLD may be related to impaired adaptive immunity to various antigens, mainly if not solely because of defective antigen processing and presentation capacities of DCs.

This is one of the first approaches to dissect the mechanisms underlying immune anomaly in NAFLD. Additional insights into the cellular and molecular mechanisms underlying antigen-specific immunity in NAFLD will help with the development of strategies to induce proper antigen-specific immunity in NAFLD subjects to tackle their susceptibility to infection and low responses to vaccination.

Acknowledgments We would like to thank the Integrated Centre for Science, Shigenobu Station, Ehime University for animal management.

References

1. Hotamisligil GS. Inflammation and metabolic disorders. Nature. 2006;444:860–7.
2. Tordjman J, Guerre-Millo M, Clément K. Adipose tissue inflammation and liver pathology in human obesity. Diabetes Metab. 2008;34:658–63.
3. Day CP, James OF. Steatohepatitis: a tale of two "hits"? Gastroenterology. 1998;114:842–5.
4. de Luca C, Olefsky JM. Inflammation and insulin resistance. FEBS Lett. 2008;582:97–105.
5. Cawthorn WP, Sethi JK. TNF-alpha and adipocyte biology. FEBS Lett. 2008;582:117–31.
6. Li Z, Soloski MJ, Diehl AM. Dietary factors alter hepatic innate immune system in mice with nonalcoholic fatty liver disease. Hepatology. 2005;42:880–5.
7. Shoelson SE, Herrero L, Naaz A. Obesity, inflammation, and insulin resistance. Gastroenterology. 2007;132:2169–80.
8. Tajiri K, Shimizu Y, Tsuneyama K, Sugiyama T. Role of liver-infiltrating CD3+ CD56+ natural killer T cells in the patogénesis of nonalcoholic fatty liver disease. Eur J Gastroenterol Hepatol. 2009;21:673–80.
9. Ma X, Hua J, Mohamood AR, Hamad AR, Ravi R, Li Z. A high-fat diet and regulatory T cells influence susceptibility to endotoxin-induced liver injury. Hepatology. 2007;46:1519–29.
10. Diehl AM. Nonalcoholic steatosis and steatohepatitis IV. Nonalcoholic fatty liver disease abnormalities in macrophage function and cytokines. Am J Physiol Gastrointest Liver Physiol. 2002;282:G1–5.
11. Nishimura S, Manabe I, Nagasaki M, Eto K, Yamashita H, Ohsugi M, et al. CD8(+) effector T cells contribute to macrophage requirement and adipose tissue inflammation in obesity. Nat Med. 2009;15:846–7.

12. Eliakim A, Schwindt C, Zaldivar F, Casali P, Cooper DM. Reduced tetanus antibody titers in overweight children. Autoimmunity. 2006;39:137–41.
13. Weber DJ, Rutala WA, Samsa GP, Bradshaw SE, Lemon SM. Impaired immunogenicity of hepatitis B vaccine in obese persons. N Engl J Med. 1986;314:1393.
14. Sanyal AJ, Contos MJ, Sterling RK, Luketic VA, Shiffman ML, Stravitz RT, et al. Nonalcoholic fatty liver disease in patients with hepatitis C is associated with features of the metabolic syndrome. Am J Gastroenterol. 2003;98:2064–71.
15. Bondini S, Kallman J, Wheeler A, Prakash S, Gramlich T, Jondle DM, et al. Impact of non-alcoholic fatty liver disease on chronic hepatitis B. Liver Int. 2007;27:607–11.
16. Rehermann B. Chronic infections with hepatotropic viruses: mechanisms of impairment of cellular immune responses. Semin Liver Dis. 2007;27:152–60.
17. Steinman RM, Banchereau J. Taking dendritic cells into medicine. Nature. 2007;449:419–26.
18. Onji M, Akbar SM. Dendritic cells in clinics. 2nd ed. Tokyo: Springer; 2008.
19. Fazle Akbar SM, Abe M, Yoshida O, Murakami H, Onji M. Dendritic cell-based therapy as a multidisciplinary approach to cancer treatment: present limitations and future scopes. Curr Med Chem. 2006;13:3113–9.
20. Niiya T, Akbar SM, Yoshida O, Miyake T, Matsuura B, Murakami H, et al. Impaired dendritic cell function resulting from chronic undernutrition disrupts the antigen-specific immune response in mice. J Nutr. 2007;137:671–5.
21. Akbar SM, Onji M, Inaba K, Yamamura K-I, Ohta Y. Low responsiveness of hepatitis B virus transgenic mice in antibody response to T-cell-dependent antigen: defect in antigen presenting activity of dendritic cells. Immunology. 1993;78:468–73.
22. Akbar SM, Inaba K, Onji M. Upregulation of MHC class II antigen on dendritic cells from hepatitis B virus transgenic mice by g-interferon: abrogation of immune response defect to a T-cell-dependent antigen. Immunology. 1996;87:519–27.
23. Akbar SM, Abe M, Masumoto T, Horiike N, Onji M. Mechanism of action of vaccine therapy in murine hepatitis B virus carriers: vaccine-induced activation of antigen presenting dendritic cells. J Hepatol. 1999;30:755–64.
24. Akbar SM, Furukawa S, Yoshida O, Hiasa Y, Horiike N, Onji M. Induction of anti-HBs in HB vaccine nonresponders in vivo by hepatitis B surface antigen-pulsed blood dendritic cells. J Hepatol. 2007;47:60–6.
25. Schaeffler A, Gross P, Buettner R, Bollheimer C, Buechler C, Neumeier M, et al. Fatty acid-induced induction of Toll-like receptor-4/nuclear factor-kappaB pathway in adipocytes links nutritional signalling with innate immunity. Immunology. 2009; 126:233–45.
26. Håversen L, Danielsson KN, Fogelstrand L, Wiklund O. Induction of proinflammatory cytokines by long-chain saturated fatty acids in human macrophages. Atherosclerosis. 2009;202:382–93.
27. Yoshida O, Akbar F, Miyake T, Abe M, Matsuura B, Hiasa Y, et al. Impaired dendritic cell functions because of depletion of natural killer cells disrupt antigen-specific immune responses in mice: restoration of adaptive immunity in natural killer-depleted mice by antigen-pulsed dendritic cell. Clin Exp Immunol. 2008; 152:174–81.
28. Coll T, Eyre E, Rodriguez-Calvo R, Palomer X, Sanchez RM, Merols M, et al. Oleate reverses palmitate-induced insulin resistance and inflammation in skeletal muscle. J Biol Chem. 2008;283:11107–16.
29. Guaraldi G, Squillace N, Stentarelli C, Orlando G, D'Amico R, Ligabue G, et al. Nonalcoholic fatty liver disease in HIV-infected patients referred to a metabolic clinic: prevalence, characteristics, and predictors. Clin Infect Dis. 2008;47:250–7.
30. Hill-Baskin AE, Markiewski MM, Buchner DA, Shao H, DeSantis D, Hsiao G, et al. Diet-induced hepatocellular carcinoma in genetically predisposed mice. Hum Mol Genet. 2009; 18:2975–88.
31. Abe M, Akbar SM, Horiike N, Onji M. Inability of liver dendritic cells from mouse with experimental hepatitis to process and present specific antigens. Hepatol Res. 2003;26:61–7.
32. Pickup JC, Crook MA. Is type II diabetes mellitus a disease of the innate immune system? Diabetologia. 1998;41:1241–8.

Contrast-Enhanced Sonography With Abdominal Virtual Sonography in Monitoring Radiofrequency Ablation of Hepatocellular Carcinoma

Yoshiyasu Kisaka, MD, Masashi Hirooka, MD, Yohei Koizumi, MD, Masanori Abe, MD, Bunzo Matsuura, MD, Yoichi Hiasa, MD, Morikazu Onji, MD

Department of Gastroenterology and Metabology, Ehime University Graduate School of Medicine, 454 Shitsukawa, Toon, Ehime 791-0295, Japan

Received 26 February 2009; accepted 28 October 2009

ABSTRACT: *Background.* Contrast-enhanced CT is regarded as the gold standard for monitoring radiofrequency ablation (RFA) of hepatocellular carcinoma (HCC). Recently, 3-dimensional volume data from CT have been used to create cross-sectional multiplanar reconstruction images. Using this technique, we can reconstruct 2-dimensional CT images identical in orientation to ultrasound (US) images, which we call virtual sonographic (VUS) images. The present prospective randomized control trial compared the number of CT scans needed to assess the efficacy of RFA of HCC using VUS-contrast-enhanced ultrasonography (CEUS) versus CT.

Method. Subjects comprised 50 patients (50 HCCs) treated with US-guided RFA between May 2005 and August 2006, randomized to undergo assessment by CT (Group 1; 25 HCC nodules) or VUS-CEUS (Group 2; 25 HCC nodules). All patients were followed for 1 year. Primary endpoint was whether the number of CT scans could be reduced using VUS-CEUS.

Result. Mean number of CT scans required was 1.64 ± 0.7 in Group 1 and 1.1 ± 0.2 in Group 2 ($p < 0.001$).

Conclusion. VUS-CEUS can be used to assess the efficacy of HCC of RFA, with the potential to reduce the number of CT scans required for that purpose. © 2009 Wiley Periodicals, Inc. *J Clin Ultrasound* **38**:138–144, 2010; Published online in Wiley InterScience (www.interscience.wiley.com). DOI: 10.1002/jcu.20654

Keywords: radiofrequency ablation; therapeutic response; virtual ultrasonography; contrast-enhanced ultrasonography; liver; hepatocellular carcinoma (HCC)

The incidence of hepatocellular carcinoma (HCC) is increasing worldwide.[1–3] Unlike other solid tumors, surgical resection plays a limited role in the treatment of HCC, as underlying cirrhosis or tumor multicentricity often contraindicates surgery.[4–6] Furthermore, HCC recurs frequently, even after curative resection.[7] Therapies such as percutaneous ethanol injection,[8–10] microwave coagulation therapy,[11,12] and radiofrequency ablation (RFA) are thus widely used in the treatment of unresectable HCC.[13–16]

RFA is frequently performed in Japan and has a higher rate of complete necrosis than other ablative procedures. For the treatment to be complete, the entire tumor must be ablated with a sufficient rim (≥5.0 mm) of noncancerous hepatic parenchyma.

Contrast-enhanced CT is the most commonly used modality for assessing the efficacy of RFA, as the ablated margin can be determined by CT both before and after RFA.[17,18] In addition, the exact ablated margin can be evaluated by injecting iodized oil (Lipiodol; Bayer, Osaka, Japan) in the tumor before RFA to delineate it subsequently (Figure 1A). CT is 1 of the most commonly used modalities for assessing the margins of the ablated volume, but it is expensive and involves potentially problematic radiation exposure.[19] Contrast-enhanced ultrasonography

Correspondence to: Y. Hiasa

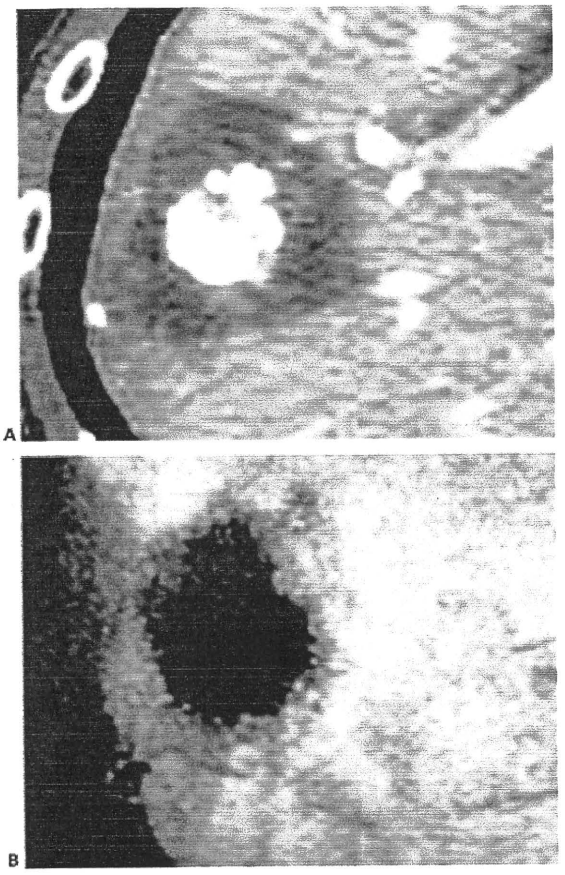

FIGURE 1. A: Post-RFA CT shows that the low-density area is larger than the ablated tumor into which iodized oil had been injected prior to RFA. The ablated margin was easily assessed, due to identification of the ablated tumor. B: In the postvascular phase on post-RFA CEUS, the ablated area appears as a homogenous unenhanced area. Ablated margins are difficult to evaluate because of the difficulty in distinguishing between ablated tumor and ablated nontumoral tissue.

(CEUS) has been reported as a useful procedure to assess the efficacy of HCC of RFA but still cannot accurately assess the ablated margins.[20]

Recently, 3-dimensional (3D) volume data from CT have been used to make cross-sectional multiplanar reconstruction images. Applying this technique, we have developed software that can reconstruct 2-dimensional CT scans identical in orientation to ultrasound scans (Virtual Place Advance software; AZE, Tokyo, Japan). We have called this technique virtual sonography (VUS).[21,22] Following RFA, the ablated margin can be assessed by comparing the VUS image of the tumor before RFA with the CEUS image showing the ablated area after RFA (VUS-CEUS) (Figure 2).

Sometimes more than 2 RFA sessions are required to ablate a HCC with a sufficient margin. In such cases, the number of CT scans required is equal to the number of sessions of RFA (Figure 3).

We therefore designed a new assessment of RFA using VUS-CEUS in replacement of CT (Figure 4). We have previously reported a retrospective study in which use of VUS-CEUS reduced the number of CT scans needed.[23] The present randomized control trial prospectively investigates the potential decrease in number of CT scans needed to assess the efficacy of RFA when VUS-CEUS is used.

PATIENTS AND METHODS

Eligibility Criteria

This study was approved by the ethics committee of the Ehime University Hospital. Between May 2005 and August 2006, a total of 50 HCCs in 50 patients were treated with US-guided percutaneous RFA. These patients were enrolled in the study after providing informed consent. All patients had to meet the following criteria for treatment with RFA: single nodular HCC $\leq$5 cm in maximum diameter; $\leq$3 lesions, each $\leq$3 cm in diameter; absence of portal venous thrombosis or extrahepatic metastases; Child-Pugh class A or B liver cirrhosis; prothrombin time >50%; and platelet count >50,000/μl. The diagnosis of HCC was confirmed by typical imaging findings, including high attenuation on CT during hepatic arteriography, and perfusion defect on CT during arterial portography. For patients with typical findings on CT during hepatic arteriography and CT during arterial portography, needle biopsy was not done.

RFA Technique

Before ablation, local anesthesia was obtained by injecting 5 ml of 1% lidocaine through the skin into the peritoneum along a predetermined puncture line. We then inserted a 20-cm-long, 17-gauge radiofrequency electrode equipped with a 2.0- or 3.0-cm-long exposed metallic tip (Cool tip; Radionics, Burlington, MA) into the tumor. If the nodule was obscured by the lungs, 500 ml saline was injected into the right pleural cavity.[24]

CT (GE Medical System, Milwaukee, WI) was performed using a Light Speed Ultra 16 scanner before RFA and at 3–5 days after treatment. Scanning parameters were as follows: 120 kVp; 175–189 mAs; 5-mm slice thickness; and table speed of 18 mm/s (pitch 0.98°) during a single

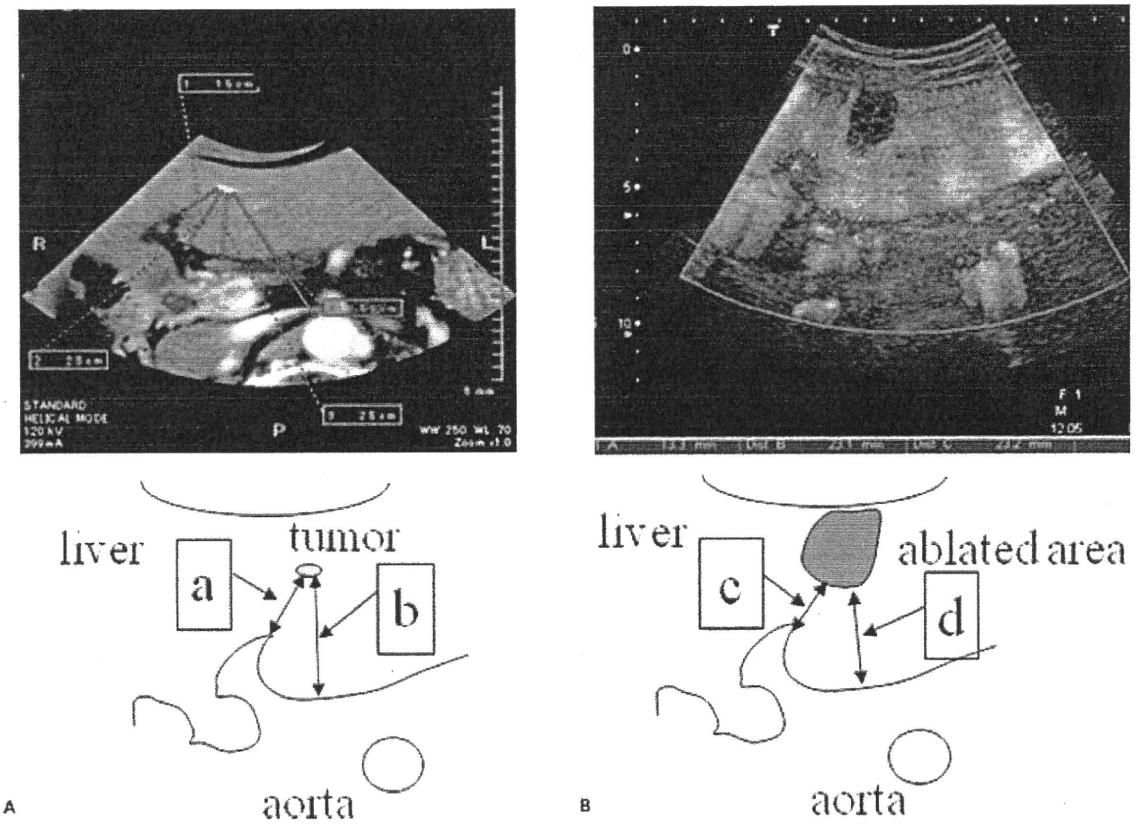

FIGURE 2. A: Assessing efficacy of RFA with VUS-CEUS. VUS shows the tumor before RFA. B: After RFA. Five minutes after injecting contrast agent (Levovist), CEUS shows the ablated area as a homogeneous unenhanced area. The difference between distances measured on VUS and on CEUS (for example, a-c, b-d in A and B) was defined as the safety margin of ablation.

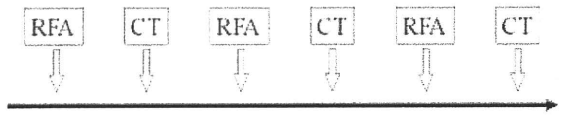

FIGURE 3. Timeline for assessing efficacy of RFA of HCC using CT (for example, in this case after 3 RFA sessions). CT was performed 3–5 days after each RFA session. The number of CT scans is equal to the number of RFA sessions.

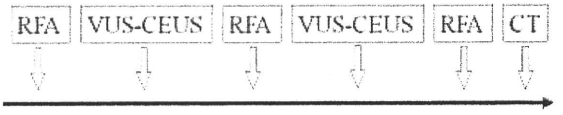

FIGURE 4. Timeline for assessing efficacy of RFA of HCC using VUS-CEUS instead of CT. VUS-CEUS was performed 3 days after each RFA session.

breath-hold helical acquisition of 7.7–10.5 seconds.

CEUS was performed 3 days after RFA using an Aplio XV system (Toshiba, Tokyo, Japan) equipped with a 4-MHz convex array transducer. The focal zone was set at the deeper margin of the tumor. Acoustic power was set at the default setting (mechanical index, 1.3–1.4). Advanced dynamic flow with a wideband Doppler technique was used, and the dynamic range for advanced dynamic flow was 40 dB. Gain was adjusted to optimize image quality in each patient. The US contrast agent used in this study was SH U 508A (Levovist; Bayer) at a dose of 300 mg/dl. The contrast was injected manually through a 20-gauge cannula into an antecubital vein at 1 ml/s. We assessed vascularity within the ablated area by means of continuous scanning at a frame rate of 5 frames/s for 10–30 seconds after injection. The ablated area was again evaluated 5 minutes after injection of US contrast medium. In this postvascular phase, the ablated area was visualized as a homogeneous nonenhanced area. Distinguishing between the ablated tumor and ablated parenchymal tissue was thus difficult. To identify the region of ablated tumor, VUS was used. For synthesis of VUS images, VUS images were generated with the software from the 3D CT volume data. It is to be noted that reconstructed VUS images are not sonograms but CT generated images that match the actual sonograms in orientation.

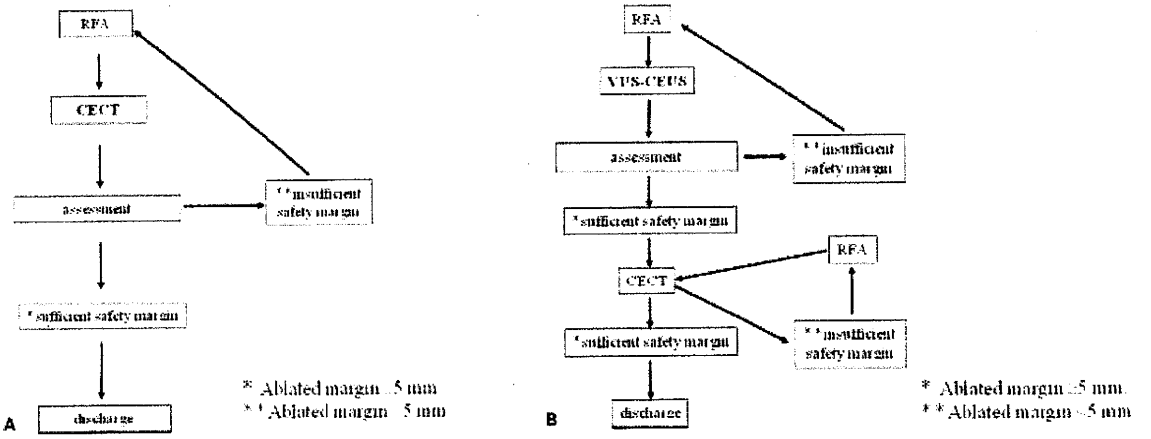

FIGURE 5. A: Assessment of efficacy of RFA of HCC with CT. If the margin is insufficient, RFA is performed again. The ablated margin is then assessed again by CT. B: Assessment of efficacy of RFA using VUS-CEUS. If the margin is insufficient, RFA is repeated. The safety margin is then assessed again by VUS-CEUS. This is continued until complete tumor ablation has been achieved. We then confirm the safety margin by CT. If the margin is insufficient, RFA is performed again. After additional RFA, efficacy is again assessed by CT.

We used anatomical landmarks to objectively measure the margins of the ablated volume. On VUS, position of the tumor was identified by measuring distance from the edge of the tumor to the anatomic landmarks (ie, surrounding organs, vessels, or edge of the liver). The same distances were also measured on CEUS scans. If the distances between the margins of the lesion and the anatomical landmarks measured on CEUS were smaller than those measured on VUS, the ablated volume was considered sufficient (Figure 2). For treatment to be complete, the entire tumor had to be ablated along with a sufficient rim of at least 5.0 mm of hepatic parenchyma. When tumors were located close (<5 mm) to the liver surface or major vessels, treatment to the adjacent parenchyma was regarded as complete ablation.

Study Design

Subjects were randomized into 2 groups of 25 cases each by computer-generated allocation with instructions in sealed envelopes to obtain 1 group of HCC treated with RFA and evaluated only by CT (Group 1) and another 1 (Group 2) evaluated with VUS-CEUS. In Group 1, efficacy of RFA was evaluated by CT as the gold standard (Figure 5A). In Group 2, VUS-CEUS was performed 3 days after each session of RFA. We performed evaluations 3 days after RFA because we wanted to evaluate not only the ablated area, but also remaining vascularity of the tumor. Vascularity could not be evaluated at 1 or 2 days after RFA, as high echogenicity persists for several hours after RFA treatment, and hypervascularity due to inflammation around the ablated area persists for 1 or 2 days. When the therapeutic effect was judged sufficient on VUS-CEUS, RFA was performed again. Three days after a second RFA, efficacy was again evaluated by VUS-CEUS. When the volume of the necrotic area was sufficient, as determined by VUS-CEUS, the lesion was evaluated by CT. If therapy was incomplete, a repeat RFA was performed. If the ablated margin was sufficient, treatment was considered complete (Figure 5B). The primary endpoint of the study was the number of CT scans needed to confirm successful RFA, and secondary endpoints were the rate of local recurrence, incidence of adverse events, and the number of treatment sessions. After treatment with RFA, serum α-fetoprotein, lectin-reactive α-fetoprotein, and plasma des-γ-carboxy-prothrombin levels were measured monthly; dynamic CT was performed after 3, 6, and 12 months, and US was performed every 3 months. Local recurrence was defined as the appearance of viable cancer adjacent to the original lesion. All patients were followed for 1 year. Major complications were defined as hemorrhage, pleural effusion requiring drainage, hepatic infarction, pneumothorax, hemothorax, bile peritonitis, liver abscess, and gastrointestinal perforation. Other complications were defined as minor complications.

Statistical Analysis

Data are expressed as mean ± SD. We calculated that a sample size of ≥22 HCCs in each group